Photochemical & Photobiological Sciences

Accepted Manuscript

This is an *Accepted Manuscript*, which has been through the Royal Society of Chemistry peer review process and has been accepted for publication.

Accepted Manuscripts are published online shortly after acceptance, before technical editing, formatting and proof reading. Using this free service, authors can make their results available to the community, in citable form, before we publish the edited article. We will replace this *Accepted Manuscript* with the edited and formatted *Advance Article* as soon as it is available.

You can find more information about *Accepted Manuscripts* in the Information for Authors.

Please note that technical editing may introduce minor changes to the text and/or graphics, which may alter content. The journal's standard Terms & Conditions and the Ethical guidelines still apply. In no event shall the Royal Society of Chemistry be held responsible for any errors or omissions in this *Accepted Manuscript* or any consequences arising from the use of any information it contains.

ROYAL SOCIETY OF CHEMISTRY

www.rsc.org/pps

Journal Name

ARTICLE

Synthesis, characterization and photophysical studies of self-assembled azo biphenyl urea derivatives

Received 00th January 20xx,
Accepted 00th January 20xx

DOI: 10.1039/x0xx00000x

www.rsc.org/

Jayaraman Sivamani, Rajendiran Balasaravanan, Kumaraguru Duraimurugan and Ayyanar Siva*

We reported to synthesize a new series of azobiphenyl based urea derivatives **7** and their stimulus-responsive supramolecular structures in the form of sheet like self assembled formations. The self-assembled nanostructure formations of azo derivatives **7** are strongly dependent on the nature of solvent present in the systems. Further, we found that the amide hydrogen played a crucial role in hydrogen bonding interactions to form a sheet like morphology upon stimulus responsive self assembly. It was confirmed by Transmission Electron Microscope and Atomic Force Microscope.

1. Introduction

Supramolecular self-assembly is of great importance for applications in material science and biology, and to achieve nanometer-scale molecular manipulations which cannot be accomplished using conventional approaches. The self-assembly of molecules into a highly ordered supramolecular structure is driven by many intermolecular forces, i.e. aromatic π–π stacking, hydrophobic forces, van der Waals forces, and hydrogen bonding interactions.[1] Self-assembly through hydrogen bonding interactions is a widely observed phenomenon in nature, because of moderately strong and directional properties.[2] The hydrogen bonding interactions between the hydrogen atom and electro negative atoms especially nitrogen and oxygen atoms has been proven to be a useful and powerful organizing force and was utilized for the formation of supramolecules.[3,4] Urea and its derivatives are ubiquitous in the biological, biochemical structures and functions and thus deserve special attention in the construction of dimensional frameworks in the recent years.[5,6]

The development of functional materials composed of macroscopic molecular assemblies that bring about reversible changes of their shape and/or physical properties with external stimuli have attracted much attention in material sciences.[7] For convenience, Light is used as an external stimulus to trigger chemical systems, photoreactions and structural isomerization's of molecules, because its intrinsically fast, easily tuneable in energy and intensity and, notably, light induced processes are often reversible.[8] Reversible control of the self-assembly of non-covalent building blocks by photo-irradiation is a key process for the synthesis of photo responsive supramolecular materials. As we know, azobenzene-type derivatives can undergo an efficient and reversible photo-isomerization reaction upon UV and visible light irradiation.[9] Therefore, photo responsive supramolecular materials based on azobenzene-typed derivatives have been widely reported in recent years, especially in supramolecular architectures could be exploited for drug delivery.[10-14]

In this context, two different biphenyl based azo molecules **7a** and **7b** containing both photo responsive azo and urea groups have been designed and synthesized in order to study the photo induced supramolecular self-assembled frameworks. (Fig. 1) Moreover, the target molecules have been explored for photo responsive behaviour and the process of supramolecular engineering in the self-assembly of molecular frameworks through aggregation studies has also been investigated. Further the self-assembled molecules are investigated by Transmission Electron Microscopy (TEM) and Atomic Force Microscopy (AFM). In the first section, we synthesized two different biphenyl based azo molecules **7** consist of two different urea moieties (**7a** and **7b**, Scheme 1) and all the compounds were well characterized by various spectral techniques such as NMR and Mass spectroscopy. In the second section, we focused on the exploration of systems engineered exclusively to undergo efficient and reversible photochemical reactions between two stable isomers featuring markedly different properties (Fig. 3, Scheme 1 and Scheme 2 in the supporting information). In the third section, we have discussed the systems self-assembled through the formation of hydrogen-bonds and that are capable of undergoing large conformational changes upon aggregation. Further, we investigated the Density Functional Theory (DFT) calculation and Cyclic Voltammetry (CV) studies for the Intramolecular Charge Transfers (ICT) of *trans* and *cis* isomers **7** (**7a**/**7b**).

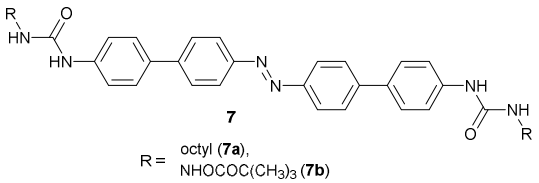

Fig. 1 Chemical structure of target molecule.

* *Department of Inorganic Chemistry, School of Chemistry, Madurai Kamaraj University, Madurai-21, Tamilnadu, India. E-mail: drasiva@gmail.com; ptcsiva@yahoo.co.in; Tel: +91451-2458471.*

†Electronic Supplementary Information (ESI) available: [details of any supplementary information available should be included here]. See DOI: 10.1039/x0xx00000x

Journal Name

ARTICLE

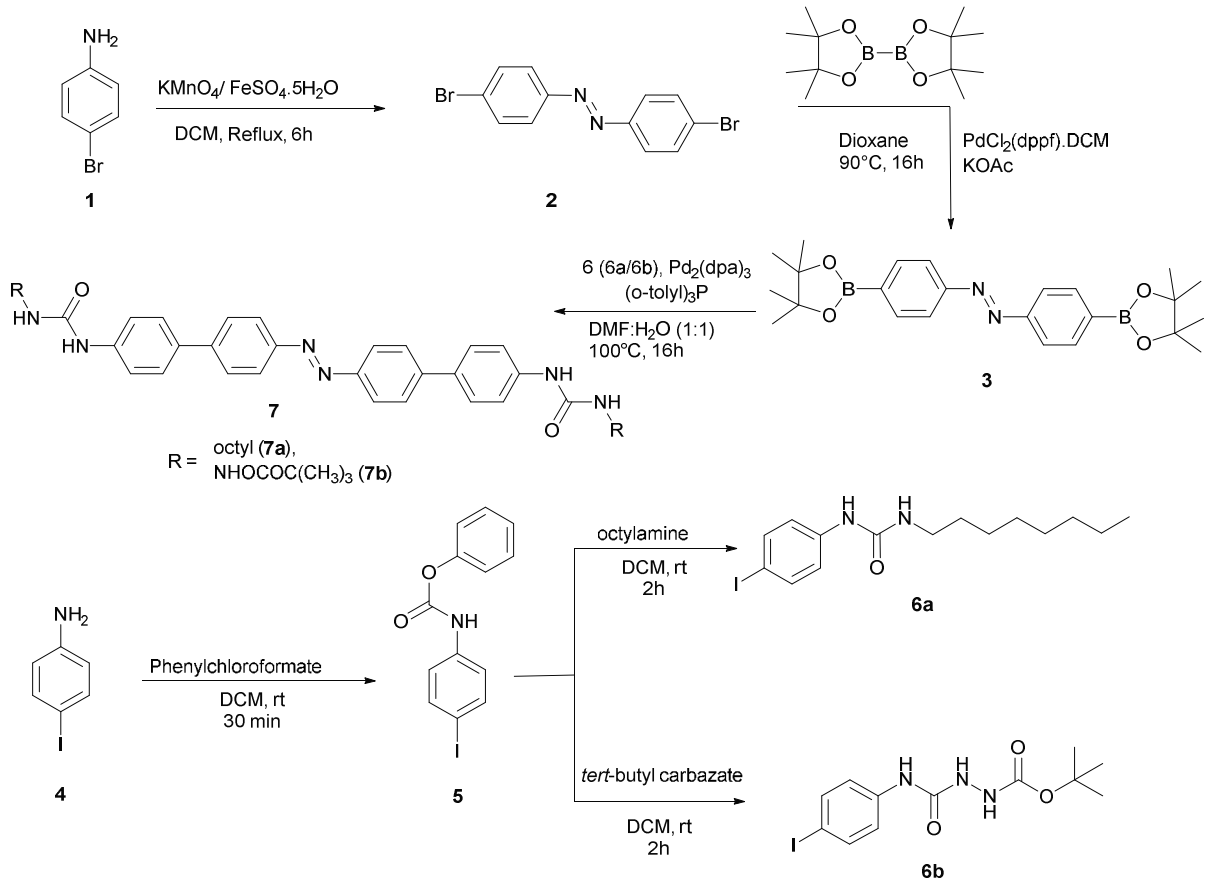

Scheme 1. Schematic representation for the synthesis of compound **7**(**7a**/**7b**).

2. Experimental section

2.1. Materials and methods

All the chemicals and reagents were used in this work as an analytical grade. 4-bromoaniline, 4-iodoaniline, phenyl chloroformate were obtained from Alfa Aesar. Bis(pincolato)diborane, $PdCl_2(PPh_3)_2$, $Pd_2(dpa)_3$ and P(*O*-Tolyl)$_3$ were obtained from Sigma Aldrich. $KMnO_4$, $FeSO_4.7H_2O$, were obtained from Merck and all the solvents were obtained from laboratory and analytical grade.

The melting points were measured in open capillary tubes and are uncorrected. The ^1H and ^{13}C NMR spectra were recorded on a Bruker (Avance) 300 & 400 MHz NMR instrument using TMS as an internal standard, $CDCl_3$ and DMSO as a solvent. Standard Bruker software was used throughout. Chemical shifts are given in parts per million (δ-scale) and the coupling constants are given in Hertz. Silica gel-G plates (Merck) were used for TLC analysis with a mixture of n-hexane and ethylacetate as an eluent. Column chromatography was carried out in silica gel (60-120 mesh) using petroleum ether and ethylacetate as an eluent. Electrospray Ionization Mass Spectrometry (ESI-MS) analyses were recorded in LCQ Fleet, Thermo Fisher Instruments Limited, US. ESI-MS was performed in positive ion mode. The collision voltage and ionization voltage were −70 V and −4.5 kV, respectively, using nitrogen as atomization and desolvation gas. The desolvation temperature was set at 300°C. The relative amount of each component was determined from the LC-MS chromatogram, using the area normalization method. UV absorption was recorded on JASCO UV-630, spectroflurometer were recorded on Agilent 8000 and photo isomerization to the *cis* isomer was performed with a Blak-Ray Long Wave Ultraviolet Lamp, Model B-100 (λ = 365 nm).[15] Cyclic voltammetry was carried out using CHI 680 electrochemical working station at RT with a scan rate of 50 mV s^{-1}. The ground-state geometries were optimized using density functional theory with

B3LYP hybrid Functional at the basis set level of 6-31G. All the calculations were performed using Gaussian 03 package. The nano aggregated sample was prepared by the following method. A stock solution of **7 (7a/7b)** in THF with the predetermined concentration of $1x10^{-4}$ M was prepared. Aliquots of the samples were transferred into 5mL volumetric flask. After adding the appropriate amount of THF, water was added drop wise under vigorous stirring to furnish $1x10^{-5}$ M solutions with different water fractions. The absorption and emission spectra of these resultant mixtures were measured immediately. All the low resolution TEM images were obtained from the deposition onto Copper grids (with carbon layer coating, 200 mesh) of dispersions (10^{-5} M) of **7** at 40% H_2O and THF; these grids were analyzed with a *Philips 208* electron microscope at a 200 kV voltage, and the resulting images were collected with an *AMT* high–resolution digital imaging camera. The 3D topography of the prepared samples was elucidated by atomic force microscopy (AFM) (Non-contact mode, A100 SGS, APE Research).

2.2. Synthesis and characterization

2.2.1. Synthesis of compound 2. Compound (**2**) was synthesized according to the procedure described in the literature.[16] 4-bromoaniline (3.5 g, 2 mmol) was taken into 250mL of the round bottom flask, dissolved in dichloromethane and in this homogeneous mixture of the oxidant (20.0 g) was added (a homogeneous mixture of the oxidant was prepared by grinding the equal amount of $KMnO_4$ (10 g) and $FeSO_4.7H_2O$ (10 g) in a mortar gently). The heterogeneous mixture was refluxed for 5 h. After the completion of the starting material, the reaction mixture was cooled to room temperature and filtered through celite, the residue washed with dichloromethane and dried over anhydrous sodium sulphate. The solvent was removed and purified by column chromatography (60-120mesh), using petroleum ether as eluent to give the corresponding compound in red solid (96% yield); mp 207°C. ^{1}H NMR (300 MHz, $CDCl_3$) δ 7.79 (d, *J* = 8.8 Hz, 4H), 7.65 (d, *J* = 8.8 Hz, 4H). ^{13}C NMR (75 MHz, $CDCl_3$) δ 151.40, 132.58, 125.98, 124.60.

2.2.2. Synthesis of compound 3. Compound (**3**) was synthesized according to the modified procedure described in the literature.[15] To a degassed solution of dry dioxane, 4, 4'-dibromoazobenzene **2** (1 g, 0.29 mmol), bis(pincolatodiborane) (2.61 g, 1.02 mmol), $PdCl_2(PPh_3)_2$ (0.052 g, 0.015 mmol, 5% mol) was added and the mixture degassed a second time. Potassium acetate (1.44 g, 1.45 mmol) was then added and the reaction mixture degassed one last time, before allowing the whole mass to stir overnight at 90°C, under nitrogen atmosphere. Then the crude mixture was filtered over celite, concentrated under vacuum and purified by Column chromatography on silica gel, using petroleum ether and ethyl acetate (5%) as eluent to give the corresponding compound in orange solid (96% yield); mp 160°C. ^{1}H NMR (300 MHz, $CDCl_3$) δ_H 7.96 (d, *J* = 8.4 Hz, 4H), 7.90 (d, *J* = 8.5 Hz, 4H), 1.37 (s, 24H). ^{13}C NMR (75 MHz, $CDCl_3$) δ_C 154.23, 135.36, 121.76, 83.18, 24.75.

2.2.3. Synthesis of compound 5. Compound (**5**) was synthesised according to the procedure described in the literature.[17] To a stirred solution of 4-iodoaniline **4** (2 g, 0.91 mmol) and pyridine (0.88 mL, 1.12 mmol) in CH_2Cl_2 at 0°C was added phenyl chloroformate (1.38 mL, 1.12 mmol) drop wise over 5 min. The mixture was stirred at 0°C for 10 min, washed with 5% aqueous citric acid, dried over anhydrous $NaSO_4$ and concentrated under vacuum. The crude material was recrystallized by toluene, to give a colourless needle in 91% yield; mp 161°C. ^{1}H NMR (300 MHz, $CDCl_3$): δ_H 7.61 (d, *J* = 8.8 Hz, 2H), 7.39 (t, *J* = 7.9 Hz, 2H), 7.25 – 7.15 (m, 5H), 6.95 (s, 1H). ^{13}C NMR (75 MHz, $CDCl_3$): δ_C 151.64, 150.62, 138.19, 137.41, 129.59, 125.98, 121.69, 120.94, 87.22.

2.3. General procedure A for synthesis of compound 6. To a stirred solution of **5** (1 eq) and Et_3N (1.1 eq) in CH_2Cl_2 at 0°C was added alkylamine (1.1 eq) drop wise over 5 min, the mixture was stirred at RT for 2 h. After the completion of the reaction, the mixture was concentrated and the crude was taken into the ether and it's stirred for 10 min, filtered and washed with ether, dried it, to get pure material.

2.3.1. Synthesis of compound 6a. Compound (**6a**) was synthesized above described general procedure A. Compound **5** (1 g, 0.29 mmol), Et_3N (0.45 mL, 0.32 mmol) and octylamine (0.54 mL, 0.32 mmol). White solid (96% yield); mp 138°C. ^{1}H NMR (400 MHz, DMSO-d_6) δ_H 8.49 (s, 1H), 7.51 (d, *J* = 8.8 Hz, 2H), 7.23 (d, *J* = 8.8 Hz, 2H), 6.14 (s, 1H), 3.05 (dd, *J* = 19.4, 6.7 Hz, 2H), 1.40 (t, *J* = 6.2 Hz, 2H), 1.25 (s, 10H), 0.85 (t, *J* = 6.6 Hz, 3H). ^{13}C NMR (100 MHz, DMSO-d_6) δ_C 154.97, 140.53, 137.15, 119.89, 83.38, 31.26, 29.70, 28.76, 28.71, 26.39, 22.11, 13.98. ESI-MS: m/z calcd for $C_{15}H_{23}IN_2O$ $[M]^+$ 374.0855; found 374.0832.

2.3.2. Synthesis of compound 6b. Compound (**6b**) was synthesized by above described general procedure A. Compound **5** (1 g, 0.29 mmol), Et_3N (0.45 mL, 0.32 mmol) and *t*-butoxycarbazate (0.43 g, 0.32 mmol). White solid (94% yield); mp 162°C. ^{1}H NMR (400 MHz, DMSO-d_6) δ_H 8.77 (s, 1H), 8.60 (s, 1H), 7.90 (s, 1H), 7.52 (d, *J* = 8.3 Hz, 2H), 7.30 (d, *J* = 7.7 Hz, 2H), 1.41 (s, 9H). ^{13}C NMR (75 MHz, DMSO-d_6) δ_C 155.91, 155.51, 139.74, 137.12, 120.65, 84.41, 79.22, 28.06. ESI-MS: m/z calcd for $C_{12}H_{16}IN_3O_3$ $[M]^+$ 377.0236; found 377.0202.

2.4. General procedure B for synthesis of compound 7 (Suzuki coupling). To a degassed solution of **3** (1 eq) in dry DMF, added K_2CO_3 (5 eq) in Water and the mixture degassed a second time. $Pd_2(dpa)_3$ (0.05 mol%) and P(*O*-Tolyl)$_3$ (0.5 mol%) was added and the mixture degassed one last time, before allowing the whole mass to stir at 100°C. To this added drop wise a degassed solution of **6** (2.2 eq) in dry DMF under the nitrogen atm, and the reaction mixture was stirred at 100°C under nitrogen atm. After the completion of the reaction mixture, the crude was filtered over celite, concentrated under vacuum and purified by Column chromatography on silica gel, using petroleum ether and ethyl acetate as eluent to give the corresponding compound **7**.

2.4.1. Synthesis of compound 7a (DPOU). Compound (**7a**) was synthesized by above described general procedure B. Compound **3** (0.3 g, 0.69 mmol), K_2CO_3 (0.48 g, 3.4 mmol), $Pd_2(dpa)_3$ (0.003 g, 0.035 mmol, 0.05 mol%), P(*O*-Tolyl)$_3$ (0.01 g, 0.35 mmol, 0.5 mol%) and **6a** (0.65 g, 1.56 mmol). Light yellow solid (67% yield); mp 105°C. ^{1}H NMR (300 MHz, DMSO-d_6) δ_H 8.37 (s, 4H), 7.36 (d, *J* = 7.6 Hz, 4H), 7.20 (t, *J* = 7.5 Hz, 4H), 6.86 (t, *J* = 7.3 Hz, 4H), 6.10 (t, *J* = 5.5 Hz, 4H), 3.05 (dd, *J* = 19.2, 6.6 Hz, 4H), 1.40 (t, *J* = 5.6 Hz, 4H), 1.25 (s, 20H), 0.85 (t, *J* = 6.0 Hz, 6H). ^{13}C NMR (75 MHz, DMSO-d_6) δ_C 155.22, 140.64, 128.61, 120.87, 117.55, 31.30, 29.81, 28.81, 28.76, 26.44, 22.14, 13.97. ESI-MS: m/z calculated for $C_{42}H_{54}N_6O_2$ $[M]^+$ 674.4308; found 674.4321.

2.4.2. Synthesis of compound 7b (DPBHU). Compound (**7b**) was synthesized by above described general procedure B. Compound **3**

(0.3 g, 0.69 mmol), K_2CO_3 (0.48 g, 3.4 mmol), $Pd_2(dpa)_3$ (0.003 g, 0.035 mmol, 0.05 mol%) , P(*O*-Tolyl)$_3$ (0.01 g, 0.35 mmol, 0.5 mol%) and **6b** (0.57 g, 1.56 mmol). Light yellow solid (65% yield); mp 138°C. ^{1}H NMR (400 MHz, DMSO-d_6) δ_H 8.82 (s, 2H), 8.66 (s, 4H), 7.98 – 7.86 (m, 4H), 7.56 (d, *J* = 8.7 Hz, 4H), 7.44 (d, *J* = 7.9 Hz, 2H), 7.31 (d, *J* = 7.8 Hz, 4H), 7.24 (t, *J* = 8.2 Hz, 2H), 1.40 (s, 18H). ^{13}C NMR (100 MHz, DMSO-d_6) δ_C 156.06, 156.00, 139.73, 137.16, 128.62, 121.78, 120.82, 79.25, 28.09. ESI-MS: m/z calcd for $C_{36}H_{40}N_8O_6$ $[M]^+$ 680.3071; found 680.3073.

3. Results and discussion

3.1. Synthesis

We have synthesized two different biphenyl based azo molecules **7** (**7a** and **7b**) consist of two different urea moieties such as octyl (**6a**) and tert-butylcarbazate (**6b**), the synthetic routes of all the compounds were depicted in scheme 1. The compounds **2**[16], **3**[15] and **5**[17] were synthesized by previously reported procedures and further, compound **5** was reacted with octylamine and *tert*-butylcarbazate to give corresponding urea **6** (**6a**/**6b**). Finally compound **3** was a Suzuki coupled with compounds **6** (**6a**/**6b**) to offered compounds **7** (**7a**/**7b**) with yield 67% (**7a**) and 65% (**7b**). All the compounds were well characterized by ^{1}H, ^{13}C NMR and mass spectra and all spectral data are given in supporting information.

3.2. Photophysical properties

The absorption and PL spectra of biphenyl based azo compounds **7a** and **7b** in THF are somewhat different to one another (Fig. 2), due to the presence of different functional groups ((3-octylurea) **6a** and (3-*tert*-butylcarbamateurea) **6b**, Scheme 1). Both the molecules exhibit two absorption maxima, attributed to the π-π* and n- π * transition of the *trans* isomer of **7**. In the absorption spectra of **7a,** absorption maxima appear at 277 nm and 370 nm, and **7b** exhibited at 293 nm and 375 nm. Compound **7b** (λ_{emi} = 392 nm, λ_{ex} = 331 nm) is exhibiting emission at higher wavelengths when compared to **7a** (λ_{emi} = 383 nm, λ_{ex} = 330 nm) due to the presence of two carbonyl groups in 7b, which in turn increase the absorption and emission values compared to 7a.

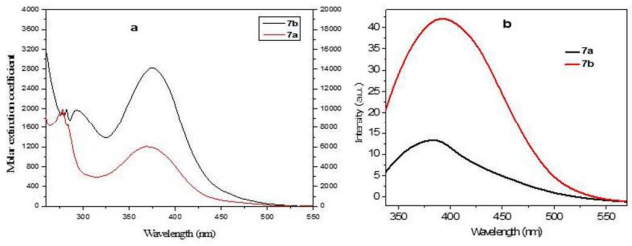

Fig. 2 Absorption (a) and PL (b) spectra of compound **7** in THF (**7a** (5 X 10^{-5} M), **7b** (1 X 10^{-5} M)).

Further, the photo physical properties of compound **7 (7a/7b)** were studied in various organic solvents (Fig. S1 and Fig. S2 in the supporting information) to find out the solvent effect and all the characteristic data were listed in Table 1 and Table 2 (in the supporting information). The polarity of solvents is strongly influenced by the photophysical properties of compounds **7 (7a/7b)**, due to the presence of the donor and acceptor groups in all the molecules. The PL spectra of compound **7 (7a/7b)** are red shifted significantly with increasing solvent polarity (Fig. S1 and Fig. S2 in the supporting information), due to increase in charge separation in the excited state, resulting in an increased dipole moment. The observed solvatochromic effects for azo derivatives **7 (7a/7b)** results from an internal charge transfer after excitation, which causes a highly polar charge separated emission state that is stabilized most effectively by polar solvents.[18] When comparing the stoke shift in all the solvents (Table 1 and Table 2 in the supporting information), it's gradually increased from non-polar to polar solvents, such behaviour is consistent with a stabilization of highly polar emitting exited state by polar solvents, i.e. the electronic redistribution occurring upon excitation.[19]

3.3. Photoisomerization

UV/Vis spectroscopy is further used to study the photo responsiveness of the incorporated azobenzenes.[20] The photo isomerization of **7** in THF is studied upon irradiation with 365 nm UV light. The absorption spectra are recorded over different time intervals until photostationary states are reached (Fig. 3). Photo isomerization from *trans*- to *cis*-azobenzene **7a** in THF (5 X 10^{-5} M) displayed absorption bands at 277 nm and 370 nm, attributed to the π-π* transition of the *cis* and *trans* isomers respectively and the band at 484 nm corresponds to the n-π* transition of the cis isomer. UV irradiation causes a progressive *trans* to *cis* isomerization as noted by the decrease of the 370 nm band and increase of the 277 nm and 484 nm band, with a photo stationary state (PSS) reached after 20 sec (Fig. 3a). A clear isobestic point was also observed at 330 nm and 448 nm. Similar reactions were also observed for **7b** (1 X 10^{-5} M), where the absorption band at 293 nm and 375 nm is attributed to the π-π* transition of the *cis* and *trans* isomers respectively, while the band at 482 nm is attributed to the n-π* transition of the cis isomer. UV irradiation causes a progressive *trans* to *cis* isomerization as noted by the decrease in intensity of π-π* band at 375 nm as the reaction proceeded, whereas the band at 293 nm and 482 are raised simultaneously, with a clear isobestic point at 331 nm and 457 nm. A photo stationary state (PSS) was reached after 20 seconds (Fig. 3b). A similar trend was also reported by Zhang,[20a] Elbing, [20b] and Liu et al. [21]

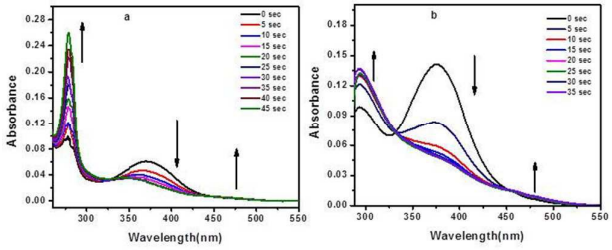

Fig. 3 Monitoring **7** shrinking upon UV irradiation (λ = 365 nm). Time evolution of the UV/Vis absorption spectra of a solution of **7** until the PSS was reached, a). **7a** in THF (in ca. 20 s, 5X10^{-5}M), b). **7b** in THF (in ca. 20 s, 1X10^{-5}M).

3.4. Aggregation studies

To determine, whether the compounds have aggregation-induced emission properties, the UV absorption and PL emission behaviours of their diluted mixtures were studied in different water–THF fractions. Compound 7 (7a/7b) is freely soluble in THF, and thereby the absorption and emission behaviour of the compound is studied through the aggregation process by increasing the percentage of water in the THF solution (Fig. S4, Fig. S3 and and Fig. S4 in the supporting information). Fig. S3 shows the emission behaviour of **7** (**7a**/**7b**) in pure THF and in THF/water mixtures. Interestingly, the increasing percentage of water (0-40%) has led to the increase in absorbance intensity and further increasing the percentage of water (50-70%) leads to decrease in absorbance. The PL spectra (Fig. 4) does not obviously show emissive with maximum at 383 nm (**7a**) and 392 nm (**7b**) in pure THF solutions, whereas with an increase in the percentage of water content from 10 to 30% (v/v), gradually the emission intensity increases with red shift as similar to absorption spectra. However the fluorescence intensity significantly increased at 40% water-THF mixture, and red shifted to 469 nm (**7a**) and 468 nm (**7b**). Furthermore, the addition of water fraction leads to a decrease in the absorption and emission intensity, we believe that in aqueous media intramolecular rotations are restricted because of the formation of nano aggregates, which block the non-radiative channels and populate the radiative excitations, thereby making the molecule emissive in their aggregated state. When the water content is increasing, the solute molecules can aggregate into two kinds of nano-particle suspensions: one is crystal particles and another one is amorphous particles. The former one result in an enhancement in the PL intensity, while the latter leads to a reduction in emission intensity.[22] A decrease in the emission intensity upon the addition of more than 40% of water fraction may be caused by the smaller number of emitting molecules which governs the fluorescence enhancement due to the restriction-in-rotation process and thereby the net fluorescence intensity is decreased for more than 40% of water-THF mixture.[23] Further the fluorescence change ensue from aggregation is indicated by the plot of fluorescence Peak intensity against corresponding water fractions (Fig. S4).

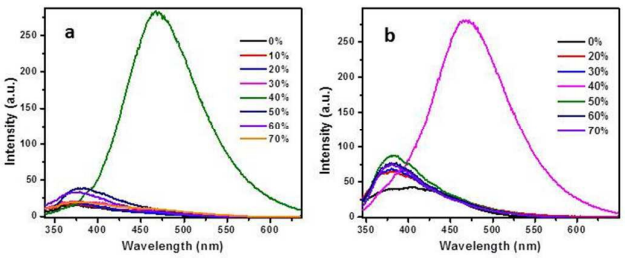

Fig. 4 Emission spectra of compound **7a** (a) and **7b** (b) in different THF: H_2O fractions excited at 330 nm and 331 nm respectively.

Moreover, these two compounds **7** (**7a**/**7b**) in 40% H_2O:THF exhibit higher fluorescence intensity and bathochromic shift when compared to those in the pure THF solution. The 40% water-THF system has the unique spectral properties in the aggregation studies. Further increasing the concentration of water 50- to 70% decrease the absorption maxima. This is due to the formation of crystalline particle of the aggregates. This can be confirmed by the electron diffraction microscopy analysis of the aggregates formed in the solvent mixtures with 40% water fraction displays many clear diffraction spots (Fig. 5, Fig. S5 in the supporting information). The studies show that the self-assembled molecules of **7a** and **7b** in 40% H_2O:THF yields nono sheets. The thickness of nano sheets are found to be approximately 30 nm for **7a** and 20 nm for **7b** (Fig. S6 in the supporting information). Furthermore, the self assembly of **7** (**7a**/**7b**) was confirmed by theoretical studies (Scheme 3; Supporting information). From these studies, we observed the formation of the sheet like (**7**) morphology through hydrogen bonding upon aggregation. The formation of hydrogen bonding was confirmed by the FT-IR spectra (Fig. S7 in the supporting information) before and after irradiation of light (365 nm).

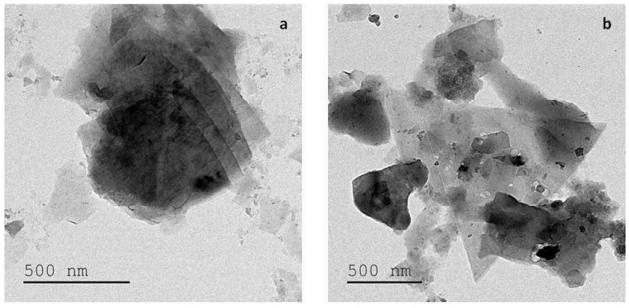

Fig. 5 TEM image of self-assembled molecules of **7a** (a) and **7b** (b) in 40% water-THF mixture.

3.5. Electrochemical experiments

Fig. 6, shows that the cyclic voltammetry (CV) diagrams of the two azo compounds **7** (**7a**/**7b**) in THF solution in the presence of 0.1 M Bu_4NBr as the supporting electrolyte with glassy carbon working electrode, platinum wire as a counter electrode and Ag/AgCl as a reference electrode at the scan rate of 50mVs^{-1}. The cyclic voltammogram of two azo compounds were recorded before and after light irradiation. From this figure (Fig. 6), we observed that both the molecules (*trans* form) exhibit good electrochemical behaviour. The oxidation and reduction peaks of **7a** at -0.63, -0.21 V and -0.346 V and **7b** at -0.67, -0.237 V and -0.25 V is observed. Further irradiation of light at 365 nm on **7** leads to decrease in both the anodic and cathodic peak current.[24] While irradiation with visible light, the original CV curves are effectively reproduced for both the compounds **7** (**7a**/**7b**).

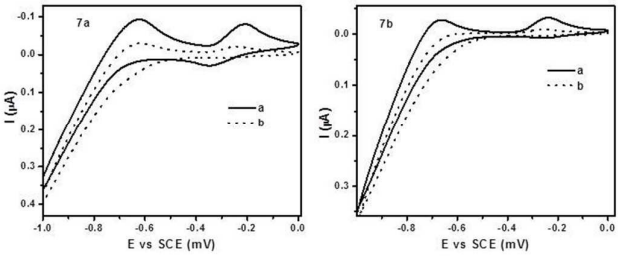

Fig. 6 Cyclic voltammograms of **7**(**7a**/**7b**) before (solid line) and after (dotted line) irradiation with wave guided 365 nm light for 20 sec. The data were obtained from measurements of the **7**(**7a**/**7b**) immersed in 0.1 M Bu_4NBr with a potential sweep rate of 50 mV between 0.0 and -1.1 V.

Journal Name

ARTICLE

3.6. Quantum chemical calculation

To investigate the geometric and electronic properties of all compounds **7** (**7a**/**7b**), quantum chemical calculations have been performed using the Gaussian 03 program.[25] The geometries of all the compounds were optimized by using the B3LYP/6-31G (d, p) functions. TDDFT calculations have been carried out using the optimized geometries, subsequently the frontier molecular orbitals were plotted. The calculated HOMO and LUMO of **7** were illustrated in Fig. 7 (**7b**) and Fig. S8 (**7a**, see in supporting information). The electron density in the HOMOs of all the compounds are mainly located on the entire pi moiety with low coefficients on the azo group, that are present in the middle of the compound **7** (**7a**/**7b**) and the LUMO is spread over mainly on the di azo linkage. The electron transition from HOMO to LUMO in all compounds are directly through intramolecular charge transfer (ICT) interactions and also due to the lowest absorption band was accompanied with a charge transfer nature of π–π* transition from the HOMO to LUMO orbital through space mechanism. In *cis*-DPOU (**7a**) the HOMO is localized over on the both biphenyl rings and the LUMO is spread over mainly on di azo linkage. In *trans*-DPOU (**7a**) the HOMO is localized over on the both biphenyl rings with the little contribution from di-azo group and the LUMO is spread over predominantly on di-azo linkage with little contribution from diphenyl units (Fig. S8 in supporting information). Thus the cause for the change in energy gap for *cis* and *trans*-DPOU (**7a**) isomers. The whole pi moiety is behaving as HOMO and the biphenyl unit with diazo unit behaving as a LUMO is in a *trans*-DPBHU (**7b**) whereas in *cis*-DPBHU (**7b**) HOMO is localized on pi moiety and diazo unit behaving as a LUMO with little contribution from one of the benzene ring (Fig. 7). These electron density changes attribute to the change in the absorption behavior of the isomers. These calculated results well coincided with the experimentally obtained results.

The TD-DFT calculations were carried out using the above mentioned sets with the optimized geometries. The absorption wavelengths and their corresponding oscillator strengths are given in Table 3 in supporting information. In this the *cis* form (**7a**) has three transitions absorbing at 466.28 nm is due to HOMO-1 to LUMO transition and 355.40, and 260.60 nm are mainly due to the HOMO to LUMO transition. The oscillator strength of the transitions is showing that these are strong transitions. In the case of *trans* form (**7a**) the absorbance wavelengths are 443.17, 374.57 and 274.39 nm, the oscillator strength of the 443.17 nm transition is weak whereas other transitions are relatively strong. The difference in oscillator strength of the *cis* and *trans* isomers related to the different photophysical behavior of the isomers. The transitions of *cis* and *trans* forms (**7b**) occur at 474.35, 363.17and 257.11 nm and 454, 367.99 and 261 nm respectively. The transitions at 474.35 and 454 nm for *cis* and *trans* are due to HOMO-1 to LUMO transition respectively and other transitions are related to the HOMO-LUMO transitions. In the case of *cis* the oscillator strength of the 474.35 nm transition is strong when compared to the *trans* form, the oscillator strength of the *trans* form is too weak.

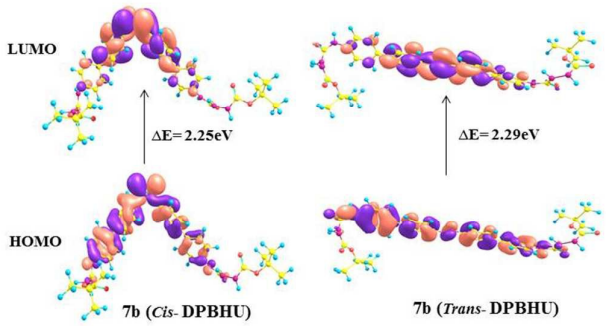

Fig. 7 DFT-computed molecular frontiers orbitals of **7b**.

4. Conclusions

In this work, we have successfully synthesized two different biphenyl based azo molecules bearing long alkyl chain and *tert*-butyl at the peripheries. These two molecules show significant photo physical properties, photo responsive studies and also exhibit self-assembly through hydrogen bonding upon aggregation to form a sheet like morphology. The electrochemical and DFT theories reveal that both the compounds exhibit intramolecular charge transfer of *trans* and *cis* isomers upon excitation.

Acknowledgments

This work was funded by the Department of Science and Technology, New Delhi, India (Grant No. SR/F/1584/2012-13) and also supported by Council of Scientific and Industrial Research, New Delhi, India (Grant No. 01(2540)/11/EMR-II).

Notes and references

1 (a) L. Brunsveld, B. Folmer, E. Meijer and R. Sijbesma, Supramolecular polymers, *Chem. Rev.*, 2001, **101**, 4071-4097; (b) T. Aida, E. Meijer and S. Stupp, Functional supramolecular polymers, *Science*, 2012, **335**, 813-817; (c) R. R. Sinden, DNA Structure and Function, Academic Press, Inc., New York, 1994; (d) J. M. Lehn, Supramolecular polymer chemistry-scope and perspectives, *Polym. Int.*, 2002, **51**, 825-839.

2 (a) L. J. Prins, D. N. Reinhoudt and P. Timmerman, Noncovalent synthesis using hydrogen bonding, *Angew. Chem. Int. Ed.*, 2001, **40**, 2382-2426; (b) G. A. Jeffrey, An introduction to hydrogen bonding, Oxford University Press, Oxford, 1997; (c) C. B. Aakeroy and K. R. Seddon, The hydrogen bond and crystal engineering, *Chem. Soc. Rev.*, 1993, **22**, 397-407; (d) J. W. Steed and J. L. Atwood, Supramolecular Chemistry, John Wiley and Sons Ltd, Chichester, 2000.

3 (a) P. S. Corbin and S. C. Zimmerman, Self-association without regard to prototropy. A heterocycle that forms extremely stable quadruply hydrogen-bonded dimers, *J. Am. Chem. Soc.*, 1998, **120**, 9710-9711; (b) P. S. Corbin and S. C. Zimmerman, Complexation-induced unfolding of heterocyclic ureas: A hydrogen-bonded, sheet like heterodimer, *J. Am. Chem. Soc.*, 2000, **122**, 3779-3780; (c) T. Park, S. C. Zimmerman, and S. Nakashima, A highly stable quadruply hydrogen-bonded heterocomplex useful for supramolecular polymer blends, *J. Am. Chem. Soc.*, 2005, **127**, 6520-6521.

4 (a) T. Park, E. M. Todd, S. Nakashima, and S. C. Zimmerman, A quadruply hydrogen bonded heterocomplex displaying high-fidelity recognition, *J. Am. Chem. Soc.*, 2005, **127**, 18133-18142; (b) Y. Yang, J. F. Xiang, M. Xue, H. Y. Hu, and C. F. Chen, Supramolecular substitution reactions between hydrazide-based molecular duplex strands: complexation induced nonsymmetry and dynamic behaviour, *J. Org. Chem.*, 2008, **73**, 6369-6377.

5 (a) G. B. W. L. Ligthart, H. Ohkawa, R. P. Sijbesma, and E. W. Meijer, Complementary quadruple hydrogen bonding in supramolecular copolymers, *J. Am. Chem. Soc.*, 2005, **127**, 810-811; (b) L. S. Shimizu, S. R. Salpage, and A. A. Korous, Functional materials from self-assembled bis-urea macrocycles, *Acc. Chem. Res.,* 2014, **47**, 2116-2127.

6 (a) P. Brocorens, M. Linares, C. G. Duhayon, R. Guillot, B. Andrioletti, D. Suhr, B. Isare, R. Lazzaroni, and L. Bouteiller, Conformational plasticity of hydrogen bonded bis-urea supramolecular polymers, *J. Phys. Chem. B*, 2013, **117**, 5379-5386; (b) K. Yabuuchi, E. M. Owusu and T. Kato, A new urea gelator: incorporation of intra-and intermolecular hydrogen bonding for stable 1D self-assembly, *Org. Biomol. Chem.*, 2003, **1**, 3464-3469.

7 (a) A. Lendlein, H. Jiang, O. Junger and R. Langer, Light-induced shape-memory polymers, *Nature*, 2005, **434**, 879-882. (b) J. Lee, C. Y. Koh, J. P. Singer, S. Jeon, M. Maldovan, O. Stein and E. L. Thomas, 25th anniversary article: ordered polymer structures for the engineering of photons and phonons, *Adv. Mater.*, 2014, **26**, 532-569; (c) S. Yagai, M. Yamauchi, A. Kobayashi, T. Karatsu, A. Kitamura, T. Ohba and Y. Kikkawa, Control over hierarchy levels in the self-assembly of stackable nanotoroids, *J. Am. Chem. Soc.*, 2012, **134**, 18205-18208; (d). V. Balzani, M. C. Leon, A. Credi, B. Ferrer, M. Venturi, A. H. Flood and J. F. Stoddart, *Proc. Natl. Acad. Sci. U. S. A.*, 2006, **103**, 1178–1183.

8 H. M. D. Bandara and S. C. Burdette, Photoisomerization in different classes of azobenzene, *Chem. Soc. Rev.*, 2012, **41**, 1809-1825.

9 S. Dawn, M. B. Dewal, D. Sobransingh, M. C. Paderes, A. C. Wibowo, M. D. Smith, J. A. Krause, P. J. Pellechia and L. S. Shimizu, Self-assembled phenylethynylene bis-urea macrocycles facilitate the selective photodimerization of coumarin, *J. Am. Chem. Soc.*, 2011, **133**, 7025-7032.

10 Y. C. Wang, J. Wu, Y. Li, J. Z. Du, Y. Y. Yuan and J. Wang, Engineering nanoscopic hydrogels via photo-crosslinking salt-induced polymer assembly for targeted drug delivery *Chem. Commun.*, 2010, **46**, 3520-3522.

11 J. Gao, Y. He, H. Xu, B. Song, X. Zhang, Z. Wang and X. Wang, Azobenzene-containing supramolecular polymer films for laser-induced surface relief gratings *Chem. Mater.*, 2007, **19**, 14-17.

12 (a) J. Gao, Y. He, F. Liu, X. Zhang, Z. Wang and X. Wang, Azobenzene-containing supramolecular side-chain polymer films for laser-induced surface relief gratings, *Chem. Mater.*, 2007, **19**, 3877-3881; (b) D. Gust, J. Andreasson, U. Pischel, T. A. Moore and A. L. Moore, Data and signal processing using photochromic molecules, *Chem. Commun.*, 2012, **48**, 1947-1957.

13 (a) X. Liang, X. Yue, Z. Dai and J. I. Kikuchi, Photoresponsive liposomal nanohybrid cerasomes, *Chem. Commun.*, 2011, **47**, 4751-7453; (b). Z. Yu and S. Hecht, Reversible and quantitative denaturation of amphiphilic oligo(azobenzene) foldamers, *Angew. Chem., Int. Ed.*, 2011, **50**, 1640-1643; (c) I. Willerich and F. Grohn, Photoswitchable nanoassemblies by electrostatic self-assembly, *Angew. Chem., Int. Ed.*, 2010, **49**, 8104-8108.

14 (a) O. Yaroshchuk and Y. Reznikov, Photoalignment of liquid crystals: basics and current trends, *J. Mater. Chem.*, 2012, **22**, 286-300; (b) W. Wu, L. Yao, T. Yang, R. Yin, F. Li and Y. Yu, NIR-light-induced deformation of cross-linked liquid-crystal polymers using upconversion nanophosphors, *J. Am. Chem. Soc.*, 2011, **133**, 15810-15813.

15 E. Busseron, J. Lux, M. Degardin and J. Rebek Jr. Synthesis and recognition studies with a ditopic, photoswitchable deep cavitand, *Chem. Commun.,* 2013, **49**, 4842-4844.

16 D. C. Barman, P. Saikia, D. Prajapati and J. S. Sandhu, Heterogeneous permanganate oxidations. a novel method for the deamination using solid supported iron-permanganate, *Synthetic Communications*, 2002, **32**, 3407-3412.

17 A. Yokoyama, T. Maruyama, K. Tagami, H. Masu, K. Katagiri, I. Azumaya, and Tsutomu Yokozawa, One-pot synthesis of cyclic triamides with a triangular cavity from *trans*-stilbene and diphenylacetylene monomers, *Org. Lett.,* **10**, 2008, 3207-3210.

18 M. H. Habibi, A. Hassanzadeh, and A. Z. Isfahani, Spectroscopic studies of solophenyl red 3BL polyazo dye tautomerism in different solvents using UV–visible, ^{1}H NMR and steady-state fluorescence techniques, *Dyes and Pigments*, 2006, **69**, 93-101.

19 J. Y. Si, K. Yang, M. Y. Jeong, H. C. Ahn, S. J. Jeon and B. R. Cho, Bis-1,4-(p-diarylaminostryl)-2,5- dicyanobenzene derivatives with large two-photon absorption cross-sections, *Org. Lett.,* 2003**, 5**, 645-648.

20 (a) J. Zhang, J. K. Whitesell and M. A. Fox, Photoreactivity of self-assembled monolayers of azobenzene or stilbene derivatives capped on colloidal gold clusters, *Chem. Mater.*, 2001, **13**, 2323-2331; (b) M. Elbing, A. Blaszczyk, C. V. Hanisch, M. Mayor, V. Ferri, C. Grave, M. A. Rampi, G. Pace, P. Samori, A. Shaporenko, and M. Zharnikov, Single component self-assembled monolayers of aromatic azo-biphenyl: influence of the packing tightness on the SAM structure and light-induced molecular movements, *Adv. Funct. Mater.*, 2008, **18**, 2972-2983.

21 (a) N. Liu, Z. Chen, D. R. Dunphy, Y. B. Jiang, R. A. Assink, and C. J. Brinker, Photoresponsive nanocomposite formed by self-assembly of an azobenzene-modified silane, *Angew. Chem. Int. Ed.*, 2003, **42**, 1731-1734.

22 Z. Y. Yang, Z. G. Chi, T. Yu, X. Q. Zhang, M. N. Chen, B. J. Xu, S. W. Liu, Y. Zhang and J. R. Xu, Triphenylethylene carbazole derivatives as a new class of AIE materials with strong blue light emission and high glass transition temperature, *J. Mater. Chem.*, 2009, **19**, 5541-5546.

23 (a) V. Bhalla, S. Kaur, V. Vij and M. Kumar, Mercury-modulated supramolecular assembly of a hexaphenylbenzene derivative for selective detection of picric acid, *Inorg. Chem.*, 2013, **52**, 4860-4865; (b) S. Dong, Z. Li, J. Qin, New carbazole-based fluorophores: synthesis, characterization, and aggregation-induced emission enhancement, *J. Phys. Chem. B*, 2009, **113**, 434-441.

24 Z. Wang, A. M. Nygard, M. J. Cook, and D. A. Russell, An evanescent-field-driven self-assembled molecular photoswitch

for macrocycle coordination and release, *Langmuir*, 2004, **20**, 5850-5857.

25 M. J. Frisch, G. W. Trucks, H. B. Schlegel, G. E. Scuseria, M. A. Robb, J. R. Cheeseman, J. A. Jr. Montgomery, T. Vreven, K. N. Kudin, J. C. Burant, J. M. Millam, S. S. Iyengar, J. Tomasi, V. Barone, B. Mennucci, M. Cossi, G. Scalmani, N. Rega, G. A. Petersson, H. Nakatsuji, M. Hada, M. Ehara, K. Toyota, R. Fukuda, J. Hasegawa, M. Ishida, T. Nakajima, Y. Honda, O. Kitao, H. Nakai, M. Klene, X. Li, J. E. Knox, H. P. Hratchian, J. B. Cross, V. Bakken, C. Adamo, J. Jaramillo, R. Gomperts, R. E. Stratmann, O. Yazyev, A. J. Austin, R. Cammi, C. Pomelli, J. W. Ochterski, P. Y. Ayala, K. Morokuma, G. A. Voth, P. Salvador, J. J. Dannenberg, V. G. Zakrzewski, S. Dapprich, A. D. Daniels, M. C. Strain, O. Farkas, D. K. Malick, A. D. Rabuck, K. Raghavachari, J. B. Foresman, J. V. Ortiz, Q. Cui, A. G. Baboul, S. Clifford, J. Cioslowski, B. B. Stefanov, G. Liu, A. Liashenko, P. Piskorz, I. Komaromi, R. L. Martin, D. J. Fox, T. Keith, M. A. A. Laham, C. Y. Peng, A. Nanayakkara, M. Challacombe, P. M. W. Gill, B. Johnson, W. Chen, M. W. Wong, C. Gonzalez and J. A. Pople, *Gaussian 03*, *Revision E.01*; *Gaussian*, *Inc*., Wallingford, CT, 2004.

Graphical Abstract

Synthesis, characterization and photophysical studies of self-assembled azo biphenyl urea derivatives

Jayaraman Sivamani, Rajendiran Balasaravanan, Kumaraguru Duraimurugan, and Ayyanar Siva*

We synthesized two different photo-responsive biphenyl azo based urea derivatives and their supramolecular self-assembled molecular frameworks through hydrogen bonding induced aggregations are reported and it's confirmed by various spectroscopy analysis.